

## Deferoxamine Mesylate

## Chemical Properties

CAS No. : 138-14-7

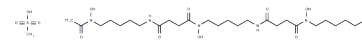
Formula: C<sub>26</sub>H<sub>52</sub>N<sub>6</sub>O<sub>11</sub>S

Molecular Weight: 656.79

Keep away from direct sunlight

Storage: Powder: -20°C for 3 years | In solvent: -80°C for 1 year

Actual storage temperature shall be subject to the COA.



## Biological Description

|               |   |
|---------------|---|
| Description   | Deferoxamine Mesylate (DFOM) is an iron chelator and ferroptosis inhibitor. Deferoxamine Mesylate binds free iron into a stable complex and reduces iron accumulation. Deferoxamine Mesylate up-regulates HIF-1 $\alpha$ levels and induces apoptosis.  |
| Targets(IC50) | Apoptosis,Mitophagy,Beta Amyloid,Ferroptosis,Reactive Oxygen Species,HIF/HIF Prolyl-Hydroxylase,Akt,Autophagy,ROS   |
| In vitro      | <p><b>METHODS:</b> Human cervical cancer cells HeLa were treated with Deferoxamine Mesylate (3-100 <math>\mu</math>M) for 72 h, and cell numbers were detected using the Incucyte HD imaging system.</p> <p><b>RESULTS:</b> Deferoxamine Mesylate inhibited cell growth in a concentration-dependent manner, and significant growth inhibition was observed at 100 <math>\mu</math>M. [1]</p> <p><b>METHODS:</b> Human colorectal cancer cells HT29 and HCT116 were treated with Deferoxamine Mesylate (50-200 <math>\mu</math>M) for 48 h, and the expression levels of target proteins were detected by Western Blot.</p> <p><b>RESULTS:</b> Deferoxamine Mesylate induced significant expression of HIF-1<math>\alpha</math> in a dose-dependent manner. [2]</p> <p><b>METHODS:</b> Human breast cancer cells MDA-MB-231 and MCF-7 were treated with Deferoxamine Mesylate (200 <math>\mu</math>M) for 24 h. Apoptosis was detected by Flow Cytometry.</p> <p><b>RESULTS:</b> After Deferoxamine Mesylate treatment, the apoptosis rate of MDA-MB-231 cells was unchanged compared with untreated cells, while apoptosis of MCF-7 cells was significantly increased. [3]</p> |
| In vivo       | <p><b>METHODS:</b> To investigate whether Deferoxamine Mesylate reduces inflammation and atherosclerosis in experimental mice, Deferoxamine Mesylate (100 mg/kg) was administered intraperitoneally to apolipoprotein E-deficient (apoE<sup>-/-</sup>) mice once a day for 10 weeks.</p> <p><b>RESULTS:</b> Deferoxamine Mesylate reduced the development of aortic atherosclerotic lesions by 26% Deferoxamine Mesylate also reduced serum MCP-1 levels and gene expression of proinflammatory and macrophage markers in the aorta and heart, and increased protein expression of transferrin receptors in the heart and liver. In contrast, Deferoxamine Mesylate treatment had no effect on serum cholesterol and triglyceride levels. [4]</p> <p><b>METHODS:</b> To study the effect of Deferoxamine Mesylate on adipocyte dysfunction in adipose tissue of ob/ob mice epididymis, Deferoxamine Mesylate (100 mg/kg) was</p>  |

|                 |   |
|-----------------|---|
| In vivo         | <p>injected intraperitoneally into ob/ob mice once daily for fifteen days.</p> <p><b>RESULTS:</b> Deferoxamine Mesylate significantly improved important parameters of adipose tissue biology by decreasing the secretion of reactive oxygen species and inflammatory markers, by increasing the levels of antioxidant enzymes, HIF-1<math>\alpha</math>, and HIF-1<math>\alpha</math>-targeted proteins, and by altering adipocyte iron-, glucose-, and lipid-related metabolic proteins. Meanwhile, hypertrophic adipocytes were reduced in size and insulin signaling pathway-related proteins were activated after Deferoxamine Mesylate treatment. [5]</p>   |
| Cell Research   | <p>After cells were seeded onto the collagen-GAG discs and allowed to adhere for 3?hours, they were placed into a hypoxic incubator with 1% O<sub>2</sub> or incubated under standard cell culture conditions with deferoxamine mesylate (DFO) added to final concentrations of 30, 60, or 120?<math>\mu</math>M. Scaffolds seeded with AdMSCs cultured under standard conditions were used as a control [3].</p>   |
| Animal Research | <p>The animals were divided into 4 groups: sham, SAH, SAH+vehicle and SAH+DFX (100mg/kg) group. DFX was administered intraperitoneally 2 and 6 hours after hemorrhage followed by every 12 hours for a maximum of 7 days. The same time course and dosage of saline were administered in the SAH+vehicle group. Afterward, rats underwent behavioral testing and were euthanized at day 1, 3, 7 and 28 for brain water content calculation, immunohistochemistry or western blot assays. The study was performed in three parts. Part 1 measured the brain water content, Evan's blue extravasation, and ultrastructural abnormalities at day 1, 3 and 7 after SAH to evaluate the time-dependent changes in brain edema and BBB disruption (n = 4 per time point and group). Part 2 investigated the role of iron in SAH-induced BBB disruption at day 1, 3 and 7 by brain water content (n = 4, per time point and group), Evan's blue extravasation (n = 4, per time point and group), transmission electron microscopy (n = 4, per time point and group), immunohistochemistry (n = 4, per time point and group) and western blot analysis (n = 3, per time point and group). Part 3 compared the acute (n = 61, per group at day 1; n = 42, per group at day 3; n = 23, per group at day 7) and long term (n = 4, per group at day 28) neurological function after SAH in each group to determine the effect of iron chelation on SAH-induced neurologic impairment [4].</p> |

### Solubility Information

|            |  |
|------------|--|
| Solubility | <p>DMSO: 127.5 mg/mL (194.13 mM),Sonication is recommended.</p> <p>H<sub>2</sub>O: 20.83 mg/mL (31.71 mM),Sonication is recommended.</p> <p>(&lt; 1 mg/ml refers to the product slightly soluble or insoluble)</p> |
|------------|--|

### Preparing Stock Solutions

---

|       | <b>1mg</b> | <b>5mg</b> | <b>10mg</b> |
|-------|------------|------------|-------------|
| 1 mM  | 1.5226 mL  | 7.6128 mL  | 15.2256 mL  |
| 5 mM  | 0.3045 mL  | 1.5226 mL  | 3.0451 mL   |
| 10 mM | 0.1523 mL  | 0.7613 mL  | 1.5226 mL   |
| 50 mM | 0.0305 mL  | 0.1523 mL  | 0.3045 mL   |

---

Please select the appropriate solvent to prepare the stock solution, according to the solubility of the product in different solvents. Please use it as soon as possible.

Note: The dilution table applies only to solid products. For liquid products, please calculate the stock solution based on the stated concentration and/or density.

## Reference

- Fujisawa K, et al. An iron chelation-based combinatorial anticancer therapy comprising deferoxamine and a lactate excretion inhibitor inhibits the proliferation of cancer cells. *Cancer Metab.* 2022 May 12;10(1):8.
- Bi G, Liang J, Shan G, et al. Retinol saturase mediates retinoid metabolism to impair a ferroptosis defense system in cancer cells. *Cancer Research.* 2023: CAN-22-3977.
- Bi G, Liang J, Zhao M, et al. MiR-6077 promotes cisplatin/pemetrexed resistance in lung adenocarcinoma by targeting CDKN1A/cell cycle arrest and KEAP1/ferroptosis pathways. *Molecular Therapy-Nucleic Acids.* 2022
- Wang S, Li F, Qiao R, et al. Arginine-Rich Manganese Silicate Nanobubbles as a Ferroptosis-Inducing Agent for Tumor-Targeted Theranostics[J]. *ACS nano.* 2018 Dec 26;12(12):12380-12392.
- Huang C Y, Chen L J, Chen G, et al. SHP-1/STAT3-Signaling-Axis-Regulated Coupling between BECN1 and SLC7A11 Contributes to Sorafenib-Induced Ferroptosis in Hepatocellular Carcinoma. *International Journal of Molecular Sciences.* 2022, 23(19): 11092.
- Sang M, Luo R, Bai Y, et al. BHQ-Cyanine-Based "Off-On" Long-Circulating Assembly as a Ferroptosis Amplifier for Cancer Treatment: A Lipid-Peroxidation Burst Device. *ACS applied materials & interfaces.* 2019, 11(46): 42873-42884.
- Wang S, Li F, Qiao R, et al. Arginine-Rich Manganese Silicate Nanobubbles as a Ferroptosis-Inducing Agent for Tumor-Targeted Theranostics. *ACS nano.* 2018 Dec 26;12(12):12380-12392.
- Fang Y, Tan Q, Zhou H, et al. Discovery and optimization of 2-(trifluoromethyl) benzimidazole derivatives as novel ferroptosis inducers in vitro and in vivo. *European Journal of Medicinal Chemistry.* 2022: 114905.
- Lv Q, Niu H, Yue L, et al. Abnormal Ferroptosis in Myelodysplastic Syndrome. *Frontiers in Oncology.* 2020 Sep 2;10: 1656
- Deng F, Xu G, Cheng Z, et al. Hepatitis B Surface Antigen Suppresses the Activation of Nuclear Factor Kappa B Pathway via Interaction With the TAK1-TAB2 Complex. *Frontiers in Immunology.* 2021, 12: 233.
- Liu Y, Li H, Luo Z, et al. Artesunate, a new antimalarial clinical drug, exhibits potent anti-AML activity by targeting the ROS/Bim and TFRC/Fe<sup>2+</sup> pathways. *British Journal of Pharmacology.* 2022
- Sang M, Luo R, Bai Y, et al. Mitochondrial membrane anchored photosensitive nano-device for lipid hydroperoxides burst and inducing ferroptosis to surmount therapy-resistant cancer. *Theranostics.* 2019, 9(21): 6209.
- Wu W Y, Wang Z X, Li T S, et al. SSBP1 drives high fructose-induced glomerular podocyte ferroptosis via activating DNA-PK/p53 pathway. *Redox Biology.* 2022: 102303.
- Zhu X, Huang N, Ji Y, et al. Brusatol induces ferroptosis in oesophageal squamous cell carcinoma by repressing GSH synthesis and increasing the labile iron pool via inhibition of the NRF2 pathway. *Biomedicine & Pharmacotherapy.* 2023, 167: 115567.
- Zhang W, et al. Deferoxamine enhances cell migration and invasion through promotion of HIF-1 $\alpha$  expression and epithelial-mesenchymal transition in colorectal cancer. *Oncol Rep.* 2014 Jan;31(1):111-6.
- Ouyang S, Li H, Lou L, et al. Inhibition of STAT3-ferroptosis negative regulatory axis suppresses tumor growth and alleviates chemoresistance in gastric cancer. *Redox Biology.* 2022: 102317
- Li X, Wang H, Lu Z, et al. Development of Multifunctional Pyrimidinylthiourea Derivatives as Potential Anti-Alzheimer Agents. *Journal of Medicinal Chemistry.* 2016 Sep 22;59(18):8326-44
- Cheng Y, Qu W, Li J, et al. Ferristatin II, an Iron Uptake Inhibitor, Exerts Neuroprotection against Traumatic Brain Injury via Suppressing Ferroptosis. *ACS Chemical Neuroscience.* 2022
- Shan G, Bi G, Zhao G, et al. Inhibition of PKA/CREB1 pathway confers sensitivity to ferroptosis in non-small cell lung cancer. *Respiratory Research.* 2023, 24(1): 1-15.
- Liu S, Tao Y, Wu S, et al. Sanguinarine chloride induces ferroptosis by regulating ROS/BACH1/HMOX1 signaling pathway in prostate cancer. *Chinese Medicine.* 2024, 19(1): 1-18.
- Ying Z, Yin M, Zhu Z, et al. Iron Stress Affects the Growth and Differentiation of *Toxoplasma gondii*. *International Journal of Molecular Sciences.* 2024, 25(5): 2493.
- Bi G, Liang J, Bian Y, et al. Polyamine-mediated ferroptosis amplification acts as a targetable vulnerability in cancer. *Nature Communications.* 2024, 15(1): 2461.
- Ru Y, Luo Y, Liu D, et al. Isorhamnetin alleviates ferroptosis-mediated colitis by activating the NRF2/HO-1 pathway and chelating iron. *International Immunopharmacology.* 2024, 135: 112318.
- Zhao G, Liang J, Zhang Y, et al. MNT inhibits lung adenocarcinoma ferroptosis and chemosensitivity by suppressing

SAT1. *Communications Biology*. 2024, 7(1): 680.

Li D, Li Y, Chen L, et al. Natural Product Auraptene Targets SLC7A11 for Degradation and Induces Hepatocellular Carcinoma Ferroptosis. *Antioxidants*. 2024, 13(8): 1015.

Chen T, Leng J, Tan J, et al. Discovery of Novel Potent Covalent Glutathione Peroxidase 4 Inhibitors as Highly Selective Ferroptosis Inducers for the Treatment of Triple-Negative Breast Cancer. *Journal of Medicinal Chemistry*. 2023

Chen C, et al. Deferoxamine Enhanced Mitochondrial Iron Accumulation and Promoted Cell Migration in Triple-Negative MDA-MB-231 Breast Cancer Cells Via a ROS-Dependent Mechanism. *Int J Mol Sci*. 2019 Oct 8;20(19):4952.

Chen R, Lin Z, Shen S, et al. Citrullination modulation stabilizes HIF-1 $\alpha$  to promote tumour progression. *Nature Communications*. 2024, 15(1): 7654.

Yang H, Dai B, Chen L, et al. Iberverin Downregulates GPX4 and SLC7A11 to Induce Ferroptotic Cell Death in Hepatocellular Carcinoma Cells. *Biomolecules*. 2024, 14(11): 1407.

Shao W, Liu F, Zhu L, et al. Ferroportin inhibits the proliferation and migration of fibroblast-like synoviocytes in rheumatoid arthritis via regulating ROS/PI3K/AKT signaling pathway. *European Journal of Pharmacology*. 2024: 177205.

Ning X, Chen X, Li R, et al. Identification of a Novel Cuproptosis Inducer That Induces ER Stress and Oxidative Stress to Trigger Immunogenic Cell Death in Tumors. *Free Radical Biology and Medicine*. 2025

Zhao G, Liang J, Shan G, et al. KLF11 regulates lung adenocarcinoma ferroptosis and chemosensitivity by suppressing GPX4. *Communications Biology*. 2023, 6(1): 570.

Zhang WJ, et al. The iron chelator, desferrioxamine, reduces inflammation and atherosclerotic lesion development in experimental mice. *Exp Biol Med (Maywood)*. 2010 May;235(5):633-41.

Yan HF, et al. Deferoxamine ameliorates adipocyte dysfunction by modulating iron metabolism in ob/ob mice. *Endocr Connect*. 2018 Apr;7(4):604-616.

Liu J, Pan Z, Tong B, et al. Artesunate protects against ocular fibrosis by suppressing fibroblast activation and inducing mitochondria-dependent ferroptosis. *The FASEB Journal*. 2023, 37(6): e22954.

Li Y, Bao Y, Li Y, et al. RSL3 Inhibits Porcine Epidemic Diarrhea Virus Replication by Activating Ferroptosis. *Viruses*. 2023, 15(10): 2080.

Duscher D, et al. Comparison of the Hydroxylase Inhibitor Dimethylxalylglycine and the Iron Chelator Deferoxamine in Diabetic and Aged Wound Healing. *Plast Reconstr Surg*. 2017 Mar;139(3):695e-706e

Gao X, Jiang P, Wei X, et al. Novel fusion protein PK5-RL-Gal-3C inhibits hepatocellular carcinoma via anti-angiogenesis and cytotoxicity. *BMC cancer*. 2023, 23(1): 1-16.

Besskaya V, Zhang H, Bian Y, et al. Hepatic nuclear factor 4 alpha promotes the ferroptosis of lung adenocarcinoma via transcriptional activation of cytochrome P450 oxidoreductase. *PeerJ*. 2023, 11: e15377.

Sang M, Luo R, Bai Y, et al. BHQ-Cyanine-Based "Off-On" Long-Circulating Assembly as a Ferroptosis Amplifier for Cancer Treatment: A Lipid-Peroxidation Burst Device[J]. *ACS applied materials & interfaces*. 2019, 11(46): 42873-42884.

Sang M, Luo R, Bai Y, et al. BHQ-Cyanine Based "Off-On" Long-Circulating Assembly as Ferroptosis Amplifier for Cancer Treatment: a Lipid-Peroxidation Burst Device[J]. *ACS applied materials & interfaces*. 2019.

Zhou Y, Wu H, Wang F, et al. GPX7 Is Targeted by miR-29b and GPX7 Knockdown Enhances Ferroptosis Induced by Erastin in Glioma. *Frontiers in oncology*. 2021, 11: 802124-802124.

**Inhibitor · Natural Compounds · Compound Libraries · Recombinant Proteins**

**This product is for Research Use Only · Not for Human or Veterinary or Therapeutic Use**

Tel: 781-999-4286 E\_mail: info@targetmol.com Address: 34 Washington Street, Wellesley Hills, MA 02481